

Dielectric relaxation and order-parameter dynamics in lawsonite

P. Sondergeld, W. Schranz, A. Tröster, and H. Kabelka

Institut für Experimentalphysik, Universität Wien, Strudlhofgasse 4, A-1090 Wien, Austria

H. Meyer and M. A. Carpenter

Department of Earth Sciences, University of Cambridge, Downing Street, Cambridge CB2 3EQ, United Kingdom

Z. Lodziana

Institute of Nuclear Physics, ul. Radzikowskiego 152, 31-342 Krakow, Poland

A. V. Kityk

Institute of Physical Optics, Dragomanova Street 23, 290005, Lviv, Ukraine

(Received 8 January 2001; published 20 June 2001)

The results of dielectric measurements ($f=10$ kHz–400 MHz) of the natural mineral lawsonite are presented in the region of the ferroelectric transition ($T_2 \approx 124$ K). The dielectric behavior is characterized by a small value of the Curie-Weiss constant ($C_{CW}=2220$ K) typical for order-disorder ferroelectrics. This is consistent with the fact that the origin of ferroelectricity in lawsonite is related to the dynamical ordering of protons. In the paraelectric phase the dielectric dispersion is characterized by a Debye relaxation with a single relaxation time $\tau_p=4.2 \times 10^{-10}(T-T_2)^{-1}$. A broadening in the dielectric dispersion occurs in the paraelectric phase only in a narrow temperature range (≈ 5 K) close to T_2 and can be associated with disordering processes in the lattice affected by large polarization clusters. The dielectric relaxation in the ferroelectric phase includes the order parameter dynamics and the domain wall dynamics. The relaxational domain wall dynamics is characterized by an extremely broad distribution of relaxation times. The characteristic parameters of the dielectric relaxation are determined.

DOI: 10.1103/PhysRevB.64.024105

PACS number(s): 77.80.Bh, 77.22.Gm, 91.60.-x

I. INTRODUCTION

Hydrogen, as a major or trace constituent of minerals has considerable influence on the physical properties of rocks and minerals. If H-containing minerals are stable to high temperatures and high pressures, they may provide an important source of hydrogen in the Earth's interior. The natural mineral lawsonite with chemical formula $\text{CaAl}_2[\text{Si}_2\text{O}_7](\text{OH})_2 \cdot \text{H}_2\text{O}$ containing $\approx 11\%$ H_2O in the structure (Fig. 1) became famous as a candidate mineral for transporting water down into the Earth's mantle at subduction zones.¹

Lawsonite undergoes two consecutive second order structural phase transitions, mainly involving changes in the positions of the H atoms and their neighbors, as well as changes in the hydrogen-bond system. At $T_1=273$ K the structure changes from $Cmcm$ (phase I) to $Pm\bar{c}n$ (phase II).^{2,3} In recent works we have extensively investigated this phase transition by means of optical, ultralow-frequency elastic, dilatometric⁴ x-ray and infrared⁵ measurements. We have observed pronounced precursor tails in all these measurements starting at temperatures of about 200 K above T_1 . The origin of these pretransitional effects is not yet understood, i.e., it is not clear if they are of intrinsic origin or defect triggered.

Below $T_2=124$ K the structure of lawsonite changes to the polar space group $P2_1cn$ (phase III).^{3,6} We have detected D - E hysteresis loops below T_2 implying that phase III is ferroelectric.⁴ First dielectric measurements yielded an increase of the dielectric permittivity ϵ_1 by a factor of 7 when

approaching T_2 from both sides. No rounding effects (except in the close vicinity of T_2) were observed, indicating that defect smearing is not important in this material and thus also the tails above T_1 are most likely of intrinsic nature. The inverse dielectric permittivity yields a linear temperature dependence above and below T_2 , but with a ratio of 1:1.25 instead of 1:2 (or 1:4 for a tricritical point) as expected from a simple Curie-Weiss law. One reason for this unusual behavior could originate from an essential contribution of mobile domain walls to the dielectric permittivity. To clarify this question, we have performed dielectric measurements of lawsonite in the extended frequency range up to 400 MHz. This extension in frequency is rather important from several viewpoints: It yields additional information about relaxational domain dynamics in the ferroelectric phase, which is expected to be suppressed in the high frequency region; the characteristic parameters for such relaxational processes can be directly obtained. Moreover the high-frequency data open the possibility to determine the parameters characterizing polarization (order parameter) dynamics. Although ferroelectricity in lawsonite is known to be related to proton ordering, we do not know much about the influence of the proton dynamics on the behavior of the polar soft mode in the vicinity of T_2 . The dielectric investigations are the first step towards an understanding of this problem.

II. EXPERIMENTAL

For the present investigation we used crystals of natural origin from Tiburon Peninsula, Marin County, California.

Structural changes

Libowitzky & Armbruster (1995):
Am. Min. **80**, 1277-1285.

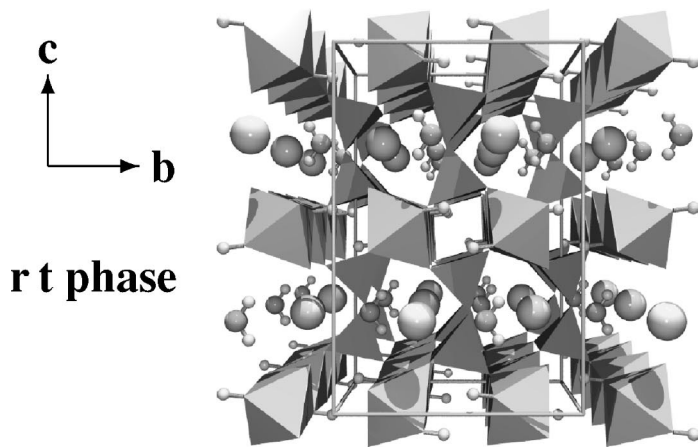
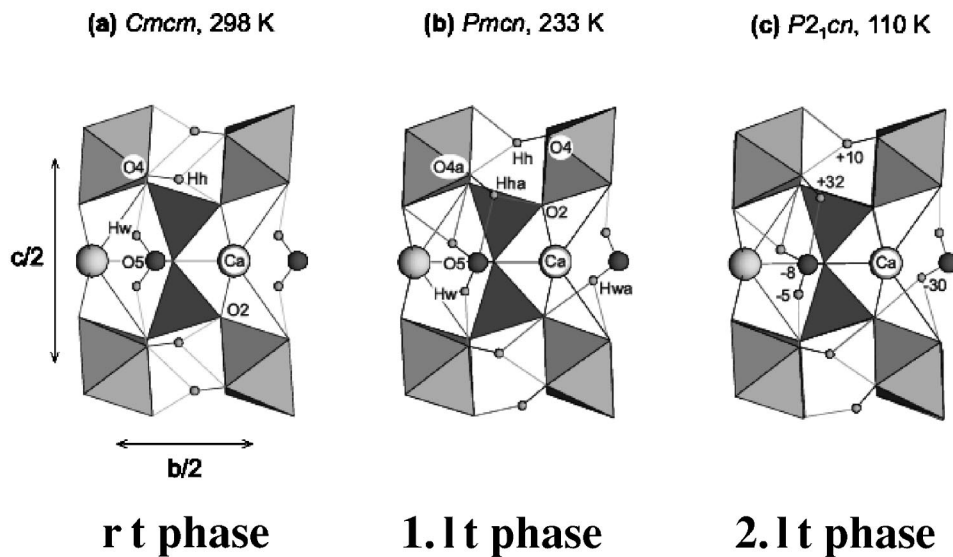


FIG. 1. Projection of the room temperature structure of lawsonite along the [100] direction. Al-O chains of octahedra are linked via Si_2O_7 units to a three-dimensional framework. The cavities are occupied by Ca^{2+} ions and water molecules.



The sample (No. G14555 of the South Australian Museum, Adelaide, Australia) was kindly provided by Dr. Allan Pring. As already described in Ref. 4 the crystals were oriented according to the natural faces and checked optically to avoid macroscopic defects, inclusions, etc. For the dielectric measurements oriented crystal plates (along the [100] direction) with thin silver painted electrodes were used. The thickness of the sample was typically 0.5 mm and the electrode area was about 10 mm². The dielectric measurements were performed combining two types of impedance analyzers manufactured by Hewlett-Packard: HP 4192A 1f in the low-

frequency range (10 kHz–1 MHz) and HP 4191A rf in the high-frequency range (1 MHz–400 MHz). In both cases the measuring process was controlled by a personal computer. The temperature of the sample chamber was regulated by a commercial temperature controller (Eurotherm 818) between 80 and 300 K.

III. EXPERIMENTAL RESULTS AND DISCUSSION

Figure 2 shows the temperature dependences of the real ϵ'_a and imaginary ϵ''_a parts of the dielectric constant of law-

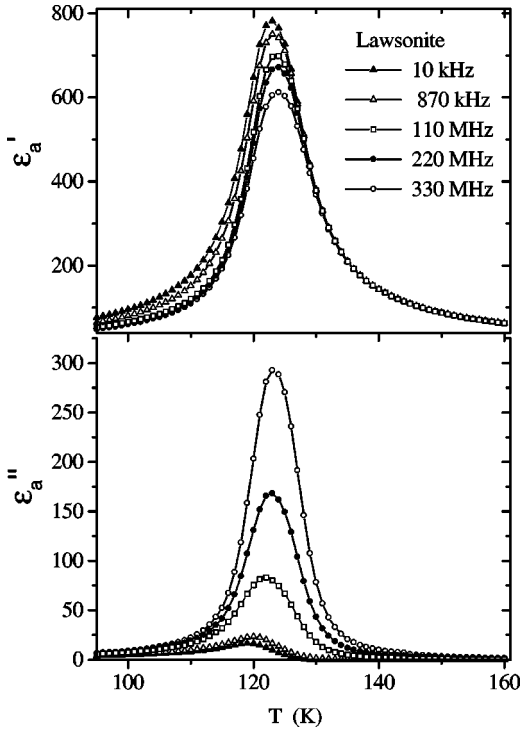


FIG. 2. Temperature dependences of the real ϵ'_a and imaginary ϵ''_a parts of the dielectric constant of lawsonite measured at different frequencies.

sonite crystals measured for different fixed frequencies. As the frequency arises the maximum in the real part ϵ'_a slightly decreases, whereas the maximum in the imaginary part ϵ''_a significantly enhances. With increasing frequencies the maxima are slightly shifted to higher temperatures. The temperature dependence of the inverse dielectric constant $1/\epsilon'_a$ for different frequencies is presented in Fig. 3.

In fact dielectric spectroscopy has been successfully applied for the study of order parameter relaxations or fluctuations,⁷ domain wall motion,^{8–10} freezing processes in glasses,^{11–13} etc., in many ferroelectric systems. Descriptions of the temperature dependence of the dielectric properties of the crystals commonly make use of the following simple Landau free energy:¹⁴

$$F = \frac{1}{2}A_0(T - T_2)P^2 + \frac{1}{4}BP^4. \quad (1)$$

In the free energy (1) the macroscopic polarization P was chosen as primary order parameter, as is usual for proper ferroelectrics.

The temperature dependence of the static inverse dielectric constant $\epsilon_p^{-1} = \partial^2 F / \partial P^2$ is given by the Curie-Weiss law

$$\begin{aligned} \epsilon_p^{-1} &= A_0(T - T_2), & T > T_2, \\ \epsilon_p^{-1} &= 2A_0(T_2 - T), & T < T_2. \end{aligned} \quad (2)$$

Comparing Eq. (2) to the experimental results presented in Fig. 3, one can draw the following conclusions.

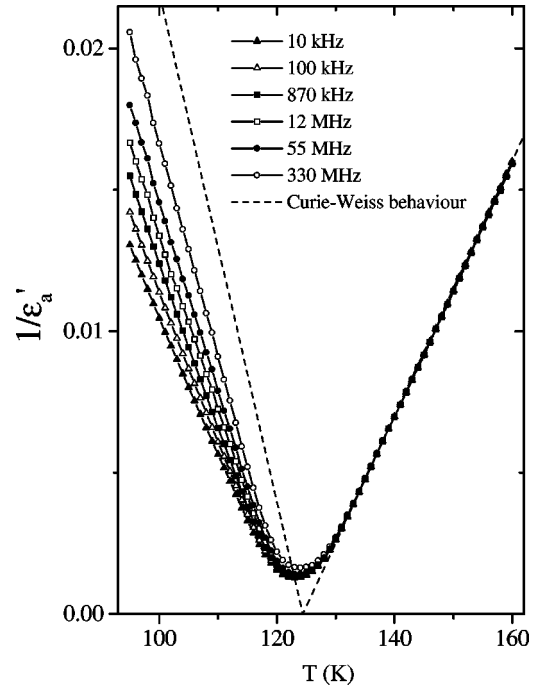


FIG. 3. Temperature dependences of the inverse dielectric constant $1/\epsilon'_a$ of lawsonite for different frequencies. The dashed line indicates the expected Curie-Weiss behavior.

(i) In the paraelectric phase II the inverse dielectric constant changes linearly with temperature, in agreement with Eq. (2). In the measured frequency range (10 kHz–330 MHz) there is practically no frequency dispersion except of a narrow temperature region (≈ 5 K) close to T_2 . The Curie-Weiss constant $C_{CW} = 1/A_0$ equals about 2220 K. This is a typical value for a wide variety of order-disorder ferroelectrics.¹⁵ Therefore the origin of ferroelectricity in lawsonite is most probably attributed to a dynamical ordering of protons rather than to their static displacements.

(ii) Equation (2) represents the Curie-Weiss law, which, as is obvious from a glance at Fig. 3, is not fulfilled. The ratio $[1/\epsilon'_a(T < T_2)]/[1/\epsilon'_a(T > T_2)]$ of slopes deviates from the predicted one (i.e., 2/1), in particular for low frequencies. As the frequency increases, the slope $1/\epsilon'_a(T)$ significantly arises approaching the expected Curie-Weiss law (dashed line in Fig. 3). To explain such a behavior the most natural assumption is the contribution of mobile domain walls to the dielectric permittivity. The influence of mobile domain walls on the dielectric response has been studied in a number of materials.^{16–18} Generally speaking, the domain wall contribution to the dielectric permittivity ϵ_D is connected with field induced shifts of the domain wall as a whole. The movement of domain walls is usually of relaxational type with a characteristic relaxation time τ_D .¹⁹ It appears to be significantly suppressed for increasing frequency, vanishing at higher frequencies (at $\omega\tau_D \gg 1$).

(iii) More details about the relaxational domain dynamics follow from the frequency dispersion curves presented in Fig. 4 for the real ϵ'_a and imaginary ϵ''_a parts. One observes that for the real part ϵ'_a the crossover region of the Debye relaxation (i.e., from $\omega\tau_D \ll 1$ to $\omega\tau_D \gg 1$) appears here in an

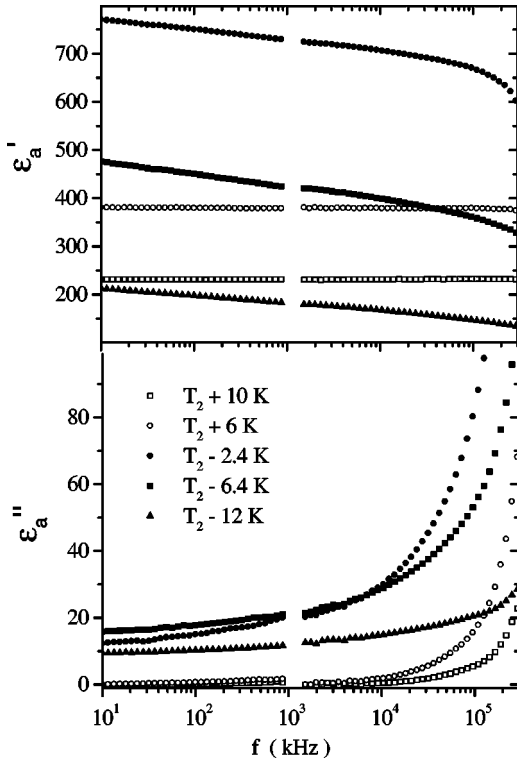


FIG. 4. Frequency dispersion of the real ϵ'_a and imaginary ϵ''_a parts of the dielectric constant of lawsonite measured at different temperatures.

extremely broad frequency range, which usually in other materials takes one or two decades. The region of this crossover cannot even be strictly determined from the presented data. In addition there is also no maximum visible in the imaginary part of the dielectric constant. One can therefore conclude that the relaxational domain dynamics in lawsonite is characterized by an extremely broad distribution of relaxation times.

The characteristic parameters of the dielectric relaxation of lawsonite, which includes order parameter (soft mode) and domain dynamics, can indeed be determined from the experimental data presented in Figs. 2–4. To account for the broadening of the dispersion it is quite suitable to describe both relaxational processes by empirical Cole-Cole relations.^{10,20,21} Then the complex dielectric constant ϵ_a^* can be written as a sum of two contributions

$$\epsilon_a^* = \frac{\epsilon_P}{1 + (i\omega\tau_P)^{\gamma_P}} + \frac{\epsilon_D}{1 + (i\omega\tau_D)^{\gamma_D}}. \quad (3)$$

ϵ_P , which is given by Eq. (2), represents the static polarization contribution to the dielectric susceptibility, ϵ_D is the domain wall contribution. In the simplest configuration of equidistant planar domain walls with average distance d and effective spring constant k , $\epsilon_D \propto P_0^2/d \cdot k$, where P_0 is the spontaneous polarization.¹⁷ τ_P and τ_D are the corresponding relaxation times, and γ_P and γ_D are the empirical exponents, which can vary in the range $0 < \gamma_D, \gamma_P \leq 1$. In its upper limit ($\gamma_D, \gamma_P = 1$) Eq. (3) transforms to the classical Debye equa-

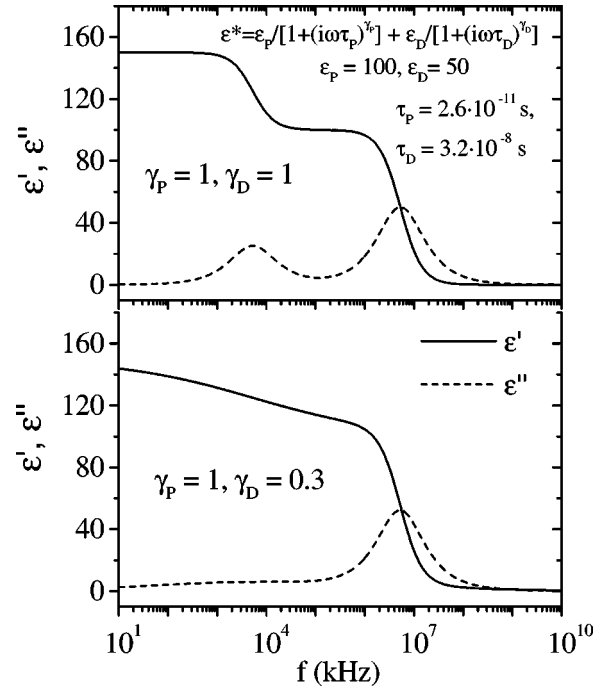
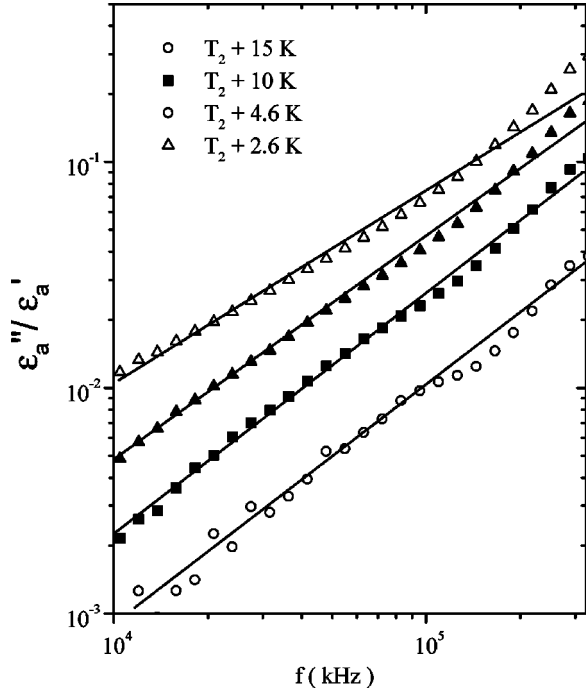


FIG. 5. Dielectric relaxation according to Eq. (3).

tion for the relaxators with single relaxation times. Figure 5 shows a plot of Eq. (3) for two different sets of parameters. One should mention that the relaxation times τ_P and τ_D are chosen here to approach reality: It is known that in many systems the order parameter relaxation time τ_P (also see the estimation below) varies in the range of about $(0.1-2) \times 10^{-10}$ s.^{22,23} τ_D is chosen to be equal 3×10^{-8} s, which corresponds to the relaxation frequency of the domain dynamics in the MHz range, i.e., a typical region for many ferroelectric materials. For comparison the domain wall relaxation in deuterated KDP occurs at a frequency of about 500 MHz and in TGS at about 5 MHz.¹⁹ For $\gamma_D = 1$ both real and imaginary parts show well separated contributions corresponding to the two Debye relaxational processes. At $\gamma_D = 0.3$ the domain contribution to the real part occurs to be smeared in an extremely wide frequency range, while the maximum in the imaginary part disappears completely. Indeed the second case appears in good qualitative agreement with the data presented in Fig. 4. As already mentioned above for $\omega\tau_D \ll 1$ the domain wall contribution to the dielectric permittivity $\epsilon_D \propto P_0^2/d \cdot k$, implying that the dielectric permittivity is enhanced due to the contribution of the mobile domain walls. This domain wall contribution increases with decreasing temperature, in good qualitative agreement with the experimental findings (Fig. 3). In this context it is remarkable that the inverse dielectric response is linear with temperature for all measured frequencies in the whole measured temperature range of the ferroelectric phase. To understand this behavior in detail a complete knowledge of the temperature dependences of the average domain wall distance and the spring constant is required.

In the paraelectric phase the domain contribution vanishes, i.e., $\epsilon_D = 0$ and the dielectric dispersion is determined

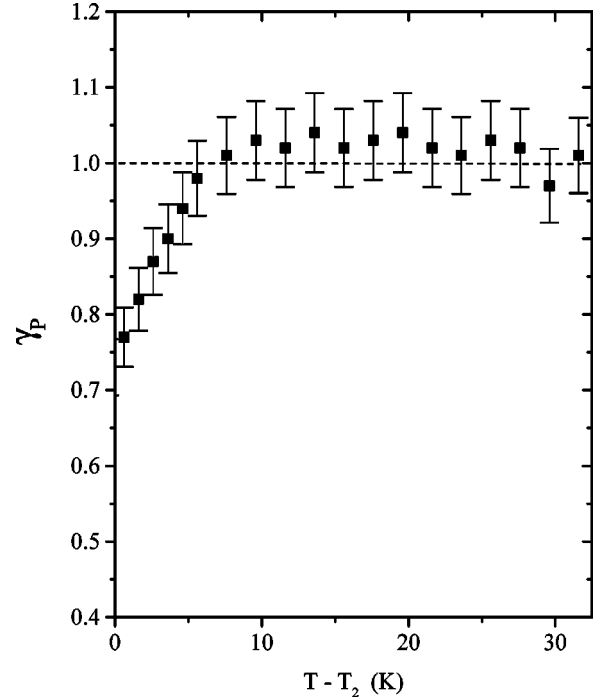
FIG. 6. Log-log plot of the ratio $\varepsilon''/\varepsilon'$ at different temperatures.

only by the first term of Eq. (3). Splitting the complex permittivity ε_a^* into real (ε'_a) and imaginary (ε''_a) parts yields

$$\frac{\varepsilon''_a}{\varepsilon'_a} = \frac{(\omega\tau_p)^{\gamma_p} \sin(\gamma_p\pi/2)}{1 - (\omega\tau_p)^{\gamma_p} \cos(\gamma_p\pi/2)}. \quad (4)$$

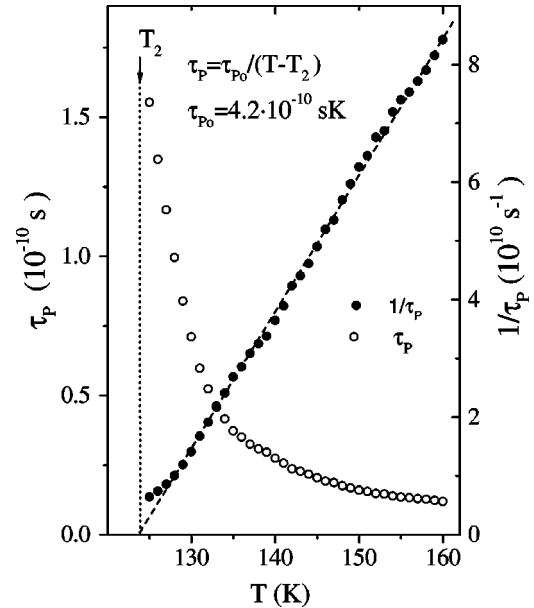
Analyzing the experimental data with the aid of Eq. (4) one can calculate the exponent γ_p at each temperature. For $\omega\tau_p \ll 1$ a log-log plot of $\varepsilon''_a/\varepsilon'_a$ versus frequency should yield a linear dependence (Fig. 6). Then the exponent γ_p can be read off from the plot. The temperature dependence of γ_p is presented in Fig. 7. One observes that well above T_2 the exponent γ_p is equal to 1. Therefore in this range the soft-mode dispersion can be characterized by a relaxator with a single relaxation time τ_p . Starting at about $T_2 + 5$ K, the exponent γ_p decreases approaching the phase transition point at T_2 . It must be stressed that since there are no domains above T_2 , the broadening of the relaxation must be attributed to large polarization clusters appearing near T_2 . Now far above T_2 the dielectric relaxation is characterized by a single relaxation time and $\omega\tau_p \ll 1$, which according to Eq. (4) yields $\tau_p = \varepsilon''_a/\varepsilon'_a \omega$. The temperature dependence of the relaxation time calculated in this way is shown in Fig. 8. The inverse relaxation time displays linear behavior in a wide temperature range, excluding a narrow region close to T_2 . This behavior can be easily reproduced within the phenomenological approach considering the relaxation equation of motion¹⁴

$$L \frac{dP}{dt} = - \frac{\partial F}{\partial P}, \quad (5)$$

FIG. 7. Temperature dependence of the exponent γ_p .

where L is a temperature independent kinetic coefficient. With the free energy (1), the temperature dependence of the inverse relaxation time is then given by

$$\begin{aligned} \tau_p^{-1} &= \frac{A_0(T - T_2)}{L}, & T > T_2, \\ \tau_p^{-1} &= \frac{2A_0(T_2 - T)}{L}, & T < T_2. \end{aligned} \quad (6)$$

FIG. 8. Temperature dependences of the order parameter relaxation time τ_p ($T > T_2$) and the inverse relaxation time $1/\tau_p$ in the paraelectric phase.

Comparing the data presented in Fig. 8 to Eq. (5), one finds for lawsonite $\tau_{P_0} = L/A_0 = 4.2 \times 10^{-10}$ s K and the kinetic coefficient $L = \tau_{P_0}/C_{CW} = 1.9 \times 10^{-13}$ s.

IV. SUMMARY

We have presented results of dielectric measurements of the mineral lawsonite in the frequency range 10 KHz–400 MHz. Summarizing the experimental data we arrive at the following conclusions.

(i) The dielectric behavior in the region of the ferroelectric transition is characterized by a small value of the Curie-Weiss constant ($C_{CW} = 2220$ K). In fact order-disorder ferroelectrics tend to have similar values of Curie-Weiss constants, i.e., $C_{CW} \approx 10^3$ K.²⁴ Also from FTIR spectroscopy it was recently suggested that the lawsonite phase transitions are of dynamic order-disorder type rather than of displacive type.⁶

(ii) We have determined the order parameter dynamics of lawsonite. The dielectric dispersion in the paraelectric phase in the region $T > T_2 + 5$ K is characterized by a Debye relaxational process with a single relaxation time varying between 10^{-11} – 10^{-10} s. Similar values for the order parameter dynamics were found for other order-disorder ferroelectrics, e.g., for KH_2PO_4 , TGS, NaNO_2 .^{7,15} A broadening in the dielectric dispersion occurs only in the narrow temperature range $T_2 < T < T_2 + 5$ K. It can be attributed to the influence of large polarization clusters which appear close to the phase transition temperature.¹⁴ The calculated inverse relaxation time shows a linear temperature dependence in the

paraelectric phase, in good agreement with the phenomenological theory.

(iii) The dielectric relaxation of lawsonite in the ferroelectric phase is more complex since it includes the order parameter (soft mode) and the domain dynamics. The relaxational domain dynamics in lawsonite is characterized by an extremely broad distribution of relaxation times, which is roughly centered around 10^{-7} – 10^{-6} s. This value can be compared with the results of other compounds. For example, in Rb_2ZnCl_4 the domain wall contribution to the dielectric permittivity was found around 0.8–3.6 MHz.¹⁷ In KH_2PO_4 crystals the domain wall dynamics occurs around 100 MHz just below $T_c = 122$ K.²⁵ The relaxation time of the dispersion increases with decreasing temperature. At about 96 K the domain wall contribution vanishes completely due to a freezing of the domain wall motion, i.e., the relaxation time diverges. We found no indication for a similar domain freezing in lawsonite down to 90 K. Measurements to lower temperatures are required to study this interesting effect in lawsonite.

ACKNOWLEDGMENTS

The present work was carried out in the frame of the EU Network on Mineral Transformations (Contract No. ERB-FMRX-CT97-0108). Support from Österreichischer Fonds zur Förderung der Wissenschaftlichen Forschung (Project No. P12226-PHY) and ÖAD-WTZ (2000-2002) is gratefully acknowledged.

¹A. R. Pawley, *Contrib. Mineral. Petrol.* **118**, 99 (1994).

²W. H. Baur, *Am. Mineral.* **63**, 311 (1978).

³E. Libowitzky and T. Ambruster, *Am. Mineral.* **80**, 1277 (1995).

⁴P. Sondergeld, W. Schranz, A. Tröster, M. A. Carpenter, E. Libowitzky, and A. V. Kityk, *Phys. Rev. B* **62**, 6143 (2000).

⁵H. W. Meyer, M. A. Carpenter, A. Graeme-Barber, P. Sondergeld, and W. Schranz, *Eur. J. Mineral.* **12**, 1139 (2000).

⁶E. Libowitzky and G. R. Rossman, *Am. Mineral.* **81**, 1080 (1996).

⁷R. Blinc and B. Zeks, in *Soft Modes in Ferroelectrics and Antiferroelectrics*, edited by E. P. Wohlfarth (North-Holland, Amsterdam, 1974).

⁸F. Gilletta, *Phys. Status Solidi A* **12**, 143 (1972).

⁹K. Kuramoto, *J. Phys. Soc. Jpn.* **56**, 1859 (1987).

¹⁰P. Kubinec, M. Fally, A. Fuith, H. Kabelka, and C. Filipic, *J. Phys.: Condens. Matter* **7**, 2205 (1995).

¹¹Z. Kutnjak, C. Filipic, A. Levstik, and R. Pirc, *Phys. Rev. Lett.* **70**, 4015 (1993).

¹²A. Levstik, C. Filipic, Z. Kutnjak, I. Levstik, R. Pirc, B. Tadic, and R. Blinc, *Phys. Rev. Lett.* **66**, 2368 (1991).

¹³P. U. T. Hochli, K. Knorr, and A. Loidl, *Adv. Phys.* **39**, 405 (1990).

¹⁴B. A. Strukov and A. P. Levanyuk, *Ferroelectric Phenomena in Crystals. Physical Foundations* (Springer-Verlag, Berlin, 1998).

¹⁵M. E. Lines and A. M. Glass, *Principle and Applications of Ferroelectrics and Related Materials* (Clarendon Press, Oxford, 1977), p. 680.

¹⁶W. Kleemann and H. Schremmer, *Phys. Rev. B* **40**, 7428 (1989).

¹⁷V. Novotna, H. Kabelka, J. Fousek, M. Havrankova, and H. Warhanek, *Phys. Rev. B* **47**, 11 019 (1993).

¹⁸R. Vana, P. Lunkenheimer, J. Hemberger, R. Böhmer, and A. Loidl, *Phys. Rev. B* **50**, 601 (1994).

¹⁹A. S. Sonin and B. A. Strukov, *Einführung in die Ferroelektrizität* (Vieweg-Verlag, Braunschweig, 1974).

²⁰K. S. Cole and R. H. Cole, *J. Chem. Phys.* **9**, 341 (1941).

²¹W. Schranz, M. Fally, and D. Havlik, *Phase Transitions* **65**, 27 (1998).

²²B. Dorner and R. Comes, in *Dynamics of Solids and Liquids by Neutron Scattering. Topics in Current Physics*, edited by S. W. Lovesey and T. Springer (Springer-Verlag, Berlin, 1977).

²³A. D. Bruce and R. A. Cowley, *Adv. Phys.* **29**, 219 (1980).

²⁴F. Jona and G. Shirane, *Ferroelectric Crystals* (Macmillan, New York, 1962).

²⁵E. Nakamura, *Ferroelectrics* **135**, 237 (1992).